SF2A 2017
C. Reylé, P. Di Matteo, F. Herpin, É. Lagadec, A. Lançon, Z. Meliani, F. Royer (eds)

CHEMICAL EVOLUTION OF THE LMC ACROSS THE FIRST KILOPARSECS

M. Van der Swaelmen[1], V. Hill[2] and F. Primas[3]

Abstract.
The LMC provides a unique laboratory to study stellar evolution and specifically nucleosynthesis at low metallicities: with its present day metallicity of only 1/3 of solar, the chemical enrichment path followed by this galaxy gives a heavy weight to the yields of metal-poor stellar generations. In order to investigate the chemical history of the LMC and constrain formation and evolution scenarios, we performed a homogeneous detailed chemical analysis of more than 250 LMC RGB stars located in three different fields: a first field located in the bar, a second in the inner disc at $\sim 2^\circ$ South of the bar, and a third in the outer parts of the LMC disc, at $\sim 4^\circ$ from the bar. Here, we present for the first time α-element abundances for the LMC outer disc field and compare it to the other two fields already investigated in our previous works: all three fields display similar trends, thus indicating a globally homogeneous chemical composition of the LMC across the first kiloparsecs.

Keywords: Stars: abundances, Galaxies: Magellanic Clouds, Galaxies: evolution, Techniques: spectroscopic

1 Introduction

Among the satellites of the Milky Way (MW), the Small and the Large Magellanic Clouds (SMC, LMC) are of particular interest since they are the closest example of galaxies in gravitational and hydrodynamical interactions. Morphological features like the Magellanic Bridge are suspected to be the signature of an LMC-SMC interaction while circum-galactic structure like the Leading Arm and the Magellanic Stream might be the result of LMC-SMC-MW interactions (*e.g.*, Besla et al. 2012). Therefore it is a unique laboratory to study in details the effect of gravitational tides and matter exchange on the chemical evolution and the star formation history of a galaxy.

The LMC is an almost face-on, gas-rich galaxy which host a bar-shaped structure at its center, embedded into an older gazeous and stellar disc. The real nature of the bar-shaped structure is still debated as it could be a dynamically-driven bar like the one found at the MW center or it could be a stellar bulge (Zaritsky 2004). Smecker-Hane et al. (2002) have derived from deep colour-magnitude diagram (CMD) the star formation histories of field stars located in the LMC bar and LMC inner disc. They show that star formation occurs at all ages. However, while the star formation history (SFH) of the bar and the inner disc are similar and rather constant at old epochs (between 7 and 14 Gy), they show that the bar has experienced a dramatic increase of its SFH, 4 to 6 Gy ago. On the contrary, Monteagudo et al. (2017) derived SFH from VIMOS data for eleven fields sampling the LMC bar and the innermost regions of the LMC disc and claim that the bar's and disc's SFH are not significantly different. Lastly, Carrera et al. (2008) showed from age-metallicity relation that the chemical composition of the LMC disc is rather homogeneous between 3° and 8°. In order to investigate the difference between the LMC bar and disc, we present here high-resolution spectroscopic abundances obtained in an homogeneous way for three different LMC fields, sampling the bar and the disc of the LMC.

[1] Institut d'Astronomie et d'Astrophysique, Université Libre de Bruxelles, Belgium
[2] Laboratoire Lagrange, UMR 7293, Université de Nice Sophia-Antipolis, Observatoire de la Côte d'Azur, BP4229, 06304, Nice Cedex 4, France
[3] European Southern Observatory, Karl Schwarzschild Str. 2, 85748 Garching b. München, Germany

2 Data

We obtained mid-resolution ($R \sim 20\,000$) mid-S/N (S/N ~ 35) spectra of LMC red giant branch stars (RGB) with the FLAMES/GIRAFFE multi-object spectrograph (Pasquini et al. 2002) of the ESO/VLT. We used three different settings HR11 ([5590, 5830] Å), HR13 ([6110, 6400] Å) and HR14 ([6290, 6690] Å). This spectral coverage of nearly 1000 Å gives us access to numerous iron lines and other atomic lines that we used to derive the metallicity, the microturbulence velocity and elemental abundances. To reduce the spectra, we used the latest version of the GIRAFFE pipeline, available through the ESO pipeline suite, *reflex*[*]. After the spectrum extraction with the GIRAFFE pipeline, we performed the sky-subtraction, radial velocity correction and co-addition of multi-epoch spectra thanks to our own set of scripts.

In this study, we compare the α-element abundances that we already obtained for 110 RGB stars located in the LMC bar (Van der Swaelmen et al. 2013) and 65 RGB stars located in the LMC inner disc (Pompéia et al. 2008; Van der Swaelmen et al. 2013) to our new set of abundances derived for RGB stars located in the LMC outer disc. This third field is located at $\sim 4°$ from the LMC center, in the vicinity of the globular cluster NGC 2210. About 90 stars of our observing program were observed with the three GIRAFFE setups. Our total sample consists of more than 250 LMC stars, that have been analysed in a homogeneous way (see next section).

3 Spectroscopic analysis

We used an iterative method to derive the atmospheric parameters of our objects, similar to the one explained in Van der Swaelmen et al. (2013). We briefly recall the main steps hereafter. The temperature is obtained thanks to the color-temperature-metallicity calibrations derived by Ramírez & Meléndez (2005). We use OGLE V & I (Ulaczyk et al. 2012) photometry and 2MASS J, H & K (Skrutskie et al. 2006) photometry which allowed the use of four photometric calibrations. On the other hand, the metallicity injected in the photometric calibrations is either an estimate (A. A. Cole, private communication) derived from the infrared Calcium II triplet index (if first iteration) or the high-resolution spectroscopic metallicity ([Fe/H]) derived from Fe I lines (subsequent iterations). The final photometric temperature is obtained by avergaging the four estimates. Then, we compute the $\log g$ using the photometric gravity formula using the photometric temperature, the metallicity and assuming a mass of $1.5 M_{\odot}$. Lastly, we fix simultaneously the metallicity and the microturbulence velocity by requiring that neutral iron lines of different equivalent widths give the same iron abundance, the equivalent widths of Fe I lines being measured with the automated tool DAOSPEC (Stetson & Pancino 2008). Most of the stars required two loops to reach convergence. Figure 1 shows the position of our stars in the H.-R. diagram.

We computed synthetic spectra by using the synthesis code *turbospectrum* (*turbospectrum* is described in Alvarez & Plez 1998 and improved along the years by B. Plez) together with the MARCS model atmosphere library (Gustafsson et al. 2008), the Gaia-ESO Survey atomic line list (Heiter et al. 2015) and molecular linelists for CN by Brooke et al. (2014); Sneden et al. (2014)[†]. We then derived elemental abundances for O, Mg, Si, Ca and Ti by absorption line fitting: we compute a grid of synthetic spectra, compare them to one observed spectrum and find the best-matching synthetic spectrum by χ^2 minimisation. The best-matching synthetic spectrum then provides the abundance of the element under study. Only two atomic lines could be used for O and Mg while about ten lines were available for Si, Ca and Ti.

4 Results & Conclusions

Figure 2 shows the abundance distributions for the five α-elements under study: O, Mg, Si, Ca and Ti. Our three LMC fields are displayed: bar (black; Van der Swaelmen et al. 2013), inner disc (red; Van der Swaelmen et al. 2013), outer disc (green; this work). The shaded area are obtained with a moving average and are an attempt to highlight the mean behaviour. We see that oxygen and magnesium have a similar behaviour: they tend to be enhanced for a metallicity [Fe/H] < -1 and then decrease to reach a solar value at a metallicity around -0.3. On the other hand, silicon, calcium and titanium tend to have a flat distribution for metallicities higher than -1.2. This difference is expected since oxygen and magnesium are produced by type II supernovae (SNII) progenitors more massive than those producing silicon, calcium and titanium.

[*] `ftp://ftp.eso.org/pub/dfs/pipelines/giraffe/giraf-pipeline-manual-2.16.pdf`

[†] Downloadable at B. Plez's webpages at `http://www.pages-perso-bertrand-plez.univ-montp2.fr/`

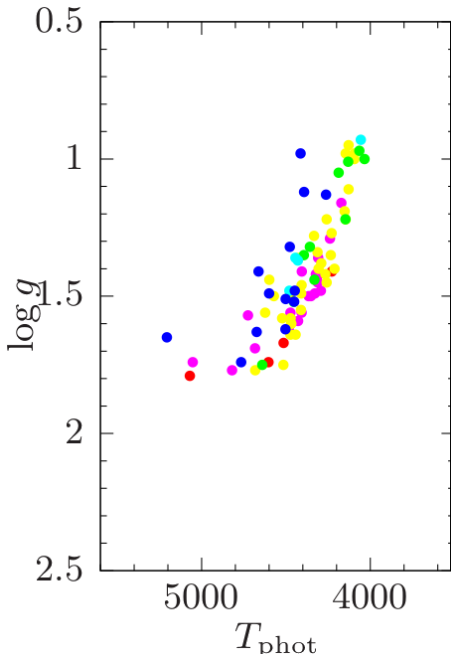

Fig. 1. Hertzsprung-Russel diagram of the LMC outer field. Metallicity bins are as follows: dark blue: [Fe/H] < -1.2; cyan: $-1.3 <$ [Fe/H] < -1.0; green: $-1.0 <$ [Fe/H] < -0.8; yellow: $-0.8 <$ [Fe/H] < -0.6; magenta: $-0.6 <$ [Fe/H] < -0.4; red: $-0.4 <$ [Fe/H].

Another feature to notice is that the abundance distributions of all fields overlap: there is no striking difference in their chemistry. This result is quite puzzling since it seems to be counterintuitive with respect to earlier results by Smecker-Hane et al. (2002) that showed a difference in the star formation history between the LMC bar and the LMC disc, which should have translated in a difference between the bar and disc α-trends. On the other hand, our abundance trends are compatible with the similar SFH derived by Monteagudo et al. (2017) for the LMC bar and disc. Thus, our results seems to speak in favour of a similar and homogeneous chemical composition of the bar and the first few kiloparsecs of the LMC disc.

Figure 3 compares our LMC α-trend (O + Mg) to that of the Milky Way (Gaia-ESO Survey Mg abundance only; see for instance Mikolaitis et al. 2014 or Kordopatis et al. 2015). Since our three LMC fields behave similary from the α-element point of view, we use a single color (red) to depict our data points. Metal-poor LMC stars possess α abundances similar to those of MW disc stars while stars with higher metallicity have α ratios smaller than that of the MW. We note also that the decrease of the [α/Fe] ratio occurs at a lower metallicity in the LMC than in the MW. This tells us that the LMC has experienced a slower chemical enrichment than that of the Milky Way and this chemical enrichment was dominated by type Ia supernovae. This could also point to a less efficient recycling of metals produced by massive SNII in the LMC. For instance, Romano & Starkenburg (2013) showed in their modelling of the Sculptor dwarf galaxy that reducing the metal recycling efficiency causes a move of the knee towards low metallicity.

To summarize, our results point at a similar and homogeneous chemical composition of the LMC bar and of the first kpc of the disc. They are compatible with the already known scenario of slow chemical enrichment of the LMC (compared to the MW) and are also compatible with a less efficient recycling of metals, which is expected for a low-mass galaxy like the LMC.

MVdS deeply thanks the SF2A for its financial support to attend “Les Journées de la SF2A”. MVdS benefits from a “Fondation ULB” fellowship.

References

Alvarez, R. & Plez, B. 1998, A&A, 330, 1109

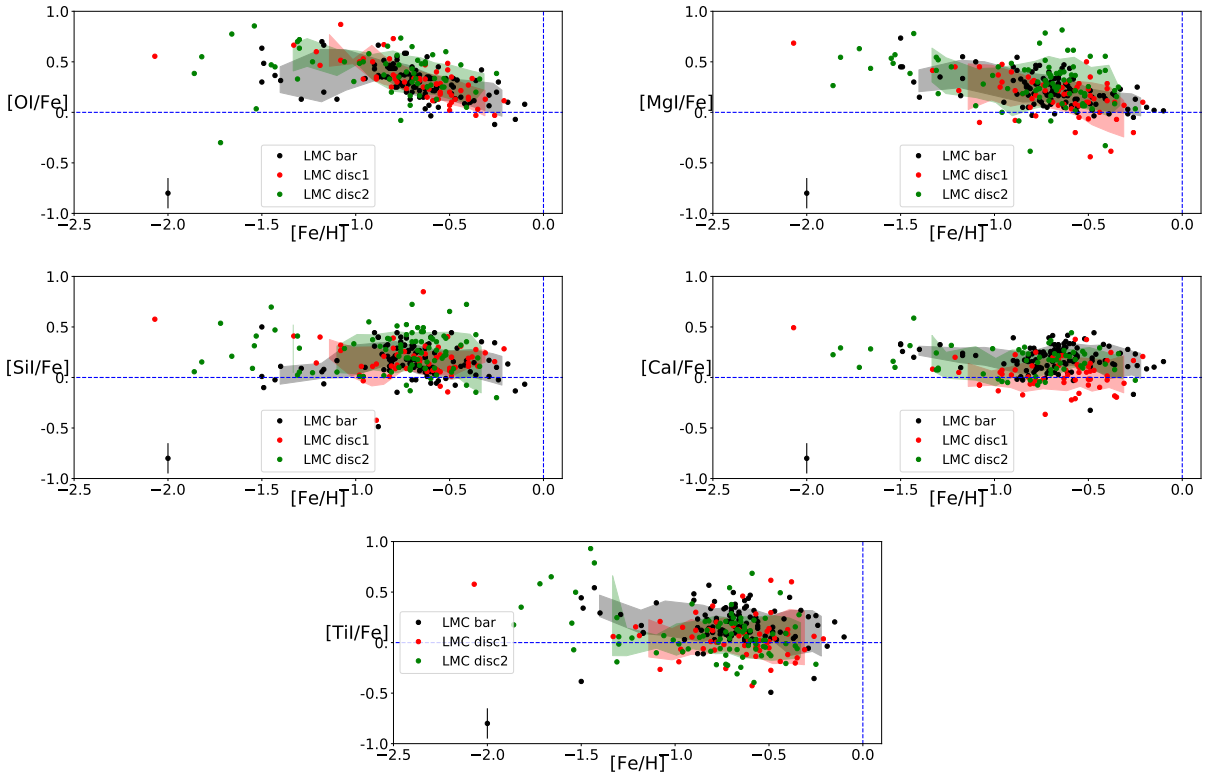

Fig. 2. Comparison of LMC O, Mg, Si, Ca, Ti trends for the three fields. Black dots: LMC bar (Van der Swaelmen et al. 2013); red dots: LMC inner disc (disc1; Van der Swaelmen et al. 2013); green dots: LMC outer disc (disc2; this work).

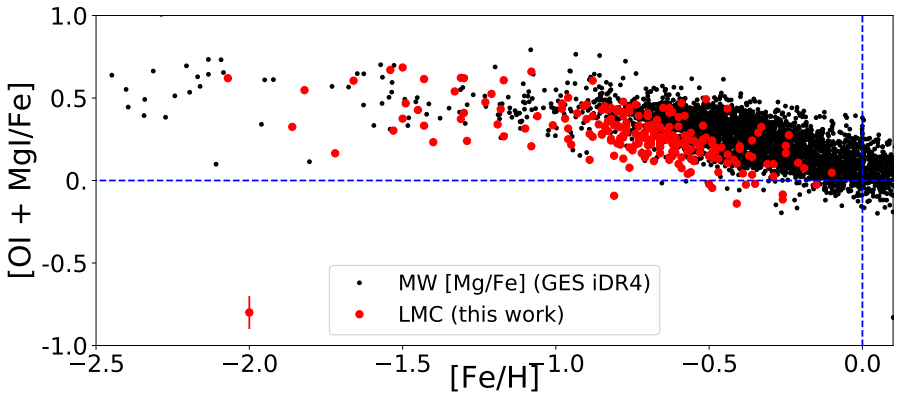

Fig. 3. Comparison of LMC [O + Mg/Fe] to MW [Mg/Fe]. Large red dots: LMC data (Van der Swaelmen et al. 2013 + this work); tiny black dots: MW GES Mg abundances.

Besla, G., Kallivayalil, N., Hernquist, L., et al. 2012, MNRAS, 421, 2109
Brooke, J. S. A., Ram, R. S., Western, C. M., et al. 2014, ApJS, 210, 23
Carrera, R., Gallart, C., Hardy, E., Aparicio, A., & Zinn, R. 2008, AJ, 135, 836
Gustafsson, B., Edvardsson, B., Eriksson, K., et al. 2008, A&A, 486, 951
Heiter, U., Lind, K., Asplund, M., et al. 2015, Phys. Scr, 90, 054010
Kordopatis, G., Wyse, R. F. G., Gilmore, G., et al. 2015, A&A, 582, A122

Mikolaitis, Š., Hill, V., Recio-Blanco, A., et al. 2014, A&A, 572, A33
Monteagudo, L., Gallart, C., Monelli, M., Bernard, E. J., & Stetson, P. B. 2017, ArXiv e-prints
Pasquini, L., Avila, G., Blecha, A., et al. 2002, The Messenger, 110, 1
Pompéia, L., Hill, V., Spite, M., et al. 2008, A&A, 480, 379
Ramírez, I. & Meléndez, J. 2005, ApJ, 626, 465
Romano, D. & Starkenburg, E. 2013, MNRAS, 434, 471
Skrutskie, M. F., Cutri, R. M., Stiening, R., et al. 2006, AJ, 131, 1163
Smecker-Hane, T. A., Cole, A. A., Gallagher, III, J. S., & Stetson, P. B. 2002, ApJ, 566, 239
Sneden, C., Lucatello, S., Ram, R. S., Brooke, J. S. A., & Bernath, P. 2014, ApJS, 214, 26
Stetson, P. B. & Pancino, E. 2008, PASP, 120, 1332
Ulaczyk, K., Szymański, M. K., Udalski, A., et al. 2012, Acta Astron., 62, 247
Van der Swaelmen, M., Hill, V., Primas, F., & Cole, A. A. 2013, A&A, 560, A44
Zaritsky, D. 2004, ApJ, 614, L37